

Journal of Biomedical Optics

SPIEDigitalLibrary.org/jbo

Monte Carlo simulation of light reflection from cosmetic powder particles near the human skin surface

Takashi Okamoto
Tatsuya Kumagawa
Masafumi Motoda
Takanori Igarashi
Keisuke Nakao

Monte Carlo simulation of light reflection from cosmetic powder particles near the human skin surface

Takashi Okamoto,^a Tatsuya Kumagawa,^a Masafumi Motoda,^a Takanori Igarashi,^b and Keisuke Nakao^b

^aKyushu Institute of Technology, Department of Systems Design and Informatics, 680-4, Kawazu, Iizuka, Fukuoka 820-8502, Japan

^bKao Corporation, Skin Beauty Research Labs., 2-1-3, Bunka, Sumida-ku, Tokyo 131-8501, Japan

Abstract. The reflection and scattering properties of light incident on human skin covered with powder particles have been investigated. A three-layer skin structure with a pigmented area is modeled, and the propagation of light in the skin's layers and in a layer of particles near the skin's surface is simulated using the Monte Carlo method. Assuming that only single scattering of light occurs in the powder layer, the simulation results show that the reflection spectra of light from the skin change with the size of powder particles. The color difference between normal and discolored skin is found to decrease considerably when powder particles with a diameter of approximately $0.25\ \mu\text{m}$ are present near the skin's surface. The effects of the medium surrounding the particles, and the influence of the distribution of particle size (polydispersity), are also examined. It is shown that a surrounding medium with a refractive index close to that of the skin substantially suppresses the extreme spectral changes caused by the powder particles covering the skin surface. © The Authors. Published by SPIE under a Creative Commons Attribution 3.0 Unported License. Distribution or reproduction of this work in whole or in part requires full attribution of the original publication, including its DOI. [DOI: 10.1117/1.JBO.18.6.061232]

Keywords: spectral reflectance; Monte Carlo method; tissue optics; powder particle; cosmetics; skin; skin discoloration.

Paper 12562SSPRR received Aug. 29, 2012; revised manuscript received Apr. 18, 2013; accepted for publication Apr. 19, 2013; published online May 22, 2013.

1 Introduction

Investigation of light propagation in human skin tissues is one of the most active topics in the field of biomedical optics, particularly in dermatology and cosmetology.¹ Light incident on skin is partly reflected from its surface, while the rest penetrates into the skin. Skin tissue consists of several layers with inhomogeneous and complicated structures, and light is scattered and absorbed as it propagates through the tissue. Some of the light, which survives absorption and multiple scattering, emerges from the skin surface as internally reflected light. Therefore, the appearance of skin is affected by both directly reflected light and internally reflected light. The complex tissue structure without some simplifications, however, prevents analytical investigation of light scattering and absorption in the skin. Intensive studies have therefore been conducted for developing computational methods to analyze the optical properties of human skin. Among the many approaches to study the interaction of light with human skin,² such as the Kubelka–Munk method,^{3,4} or the Monte Carlo (MC) method, the MC method is a powerful tool to analyze photon propagation in such scattering media.^{5–12} The MC method has proven to be useful in obtaining the spectrum and spatial distribution of light reflected from the bare skin. In some applications, however, one has to deal with situations in which cosmetic powder or sunscreen is also applied to the skin.

In spite of its usefulness, only few investigations have utilized the MC method to examine the effect of such particulate scatterers and absorbers on and in the skin; notable exceptions include the research of Lademann, Popov and colleagues,^{13–16} who studied the ultraviolet (UV) protection properties of

nanoparticles using MC simulations. Since the MC method has not been fully utilized yet in cosmetology, it is desirable to investigate the effect of foundation makeup on the appearance of the face using this computational simulation method. In order to design cosmetic foundations that give better skin appearance, the reflection and scattering properties of light incident on facial skin covered with cosmetic powders need to be analyzed. In particular, it is important to elucidate the effect of powder particles on light reflection from wrinkles, pores, freckles, spots, and blemishes, since obscuring skin imperfections is one of the important purposes of foundation makeup.

In this study, we investigate the reflection and scattering properties of light incident on skin covered with cosmetic powders. While nanoparticles in sunscreen for UV protection are so small that they go into the stratum corneum,^{13–16} cosmetic foundations mainly consist of submicrometer to micrometer particles and stay on or near the skin surface. In our investigations, a three-layered skin tissue with discoloration is modeled, and the propagation of light through the skin and the scattering of light by particles near the skin surface are simulated by means of the MC method. It is shown that the spectral reflectance and the color image of the skin depend strongly on the size of powder particles. The effect of size distribution of particles on the spectrum and color of light is also investigated and analyzed.

2 Simulation Method

Figure 1 shows a simulation model used in this study. As a skin tissue model, we employed a trilaminar structure consisting of the epidermis, dermis, and subcutis. The refractive index was assumed to be 1.4 for all the layers, and the absorption (μ_a) and scattering (μ_s) coefficients and the anisotropy factor g appropriate for each layer were chosen for each wavelength of light in the visible portion of the spectrum, ranging from 400 to 780 nm (see Fig. 2 and Appendix A).¹⁷ Spherical particles of rutile-type titanium dioxide (TiO_2) with a specific

Address all correspondence to: Takashi Okamoto, Kyushu Institute of Technology, Department of Systems Design and Informatics, 680-4, Kawazu, Iizuka, Fukuoka 820-8502, Japan. Tel: +81 948 29 7725; Fax +81 948 29 7725; E-mail: okamoto@ces.kyutech.ac.jp

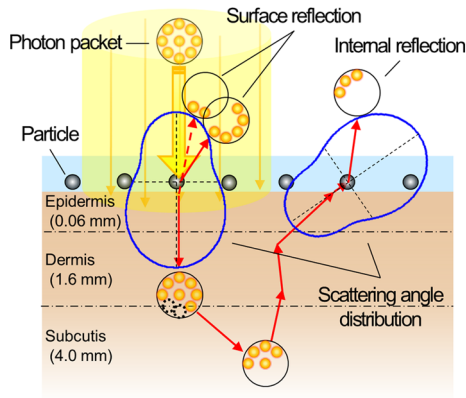


Fig. 1 Schematic diagram of the skin for the simulation model.

weight of 4.26 g/cm^3 were assumed to be used as powder particles that cover the skin surface. The refractive index of the particles is plotted in Fig. 3(a), which was calculated according to the equations in Ref. 18. The optical properties of the particles we used in the simulation are shown in Fig. 3(b)–3(e) (see Appendix A). The concentration of the particles is set to be $5.39 \mu\text{g/cm}^2$; this value is small compared with the usual concentration of powders in makeup foundations, which is about 0.1 to 0.2 mg/cm^2 . In our simulation, we are interested in the single scattering component of light, which best describes the scattering characteristics of each particle size. The effect of multiple scattering is significant for the optical depth to be larger than 1. We found the concentration value by calculating the maximum concentration of particles allowable under the condition that the optical depth of the particle layer is less

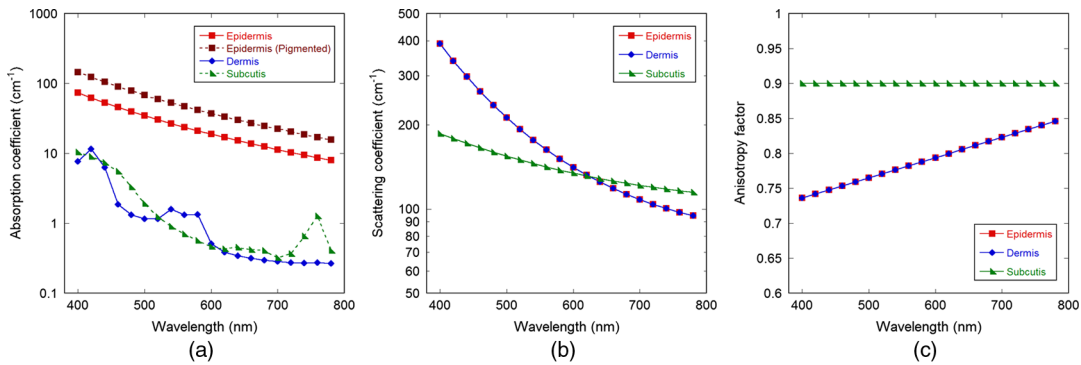


Fig. 2 (a) Absorption coefficient, (b) scattering coefficient, and (c) anisotropy factor g .

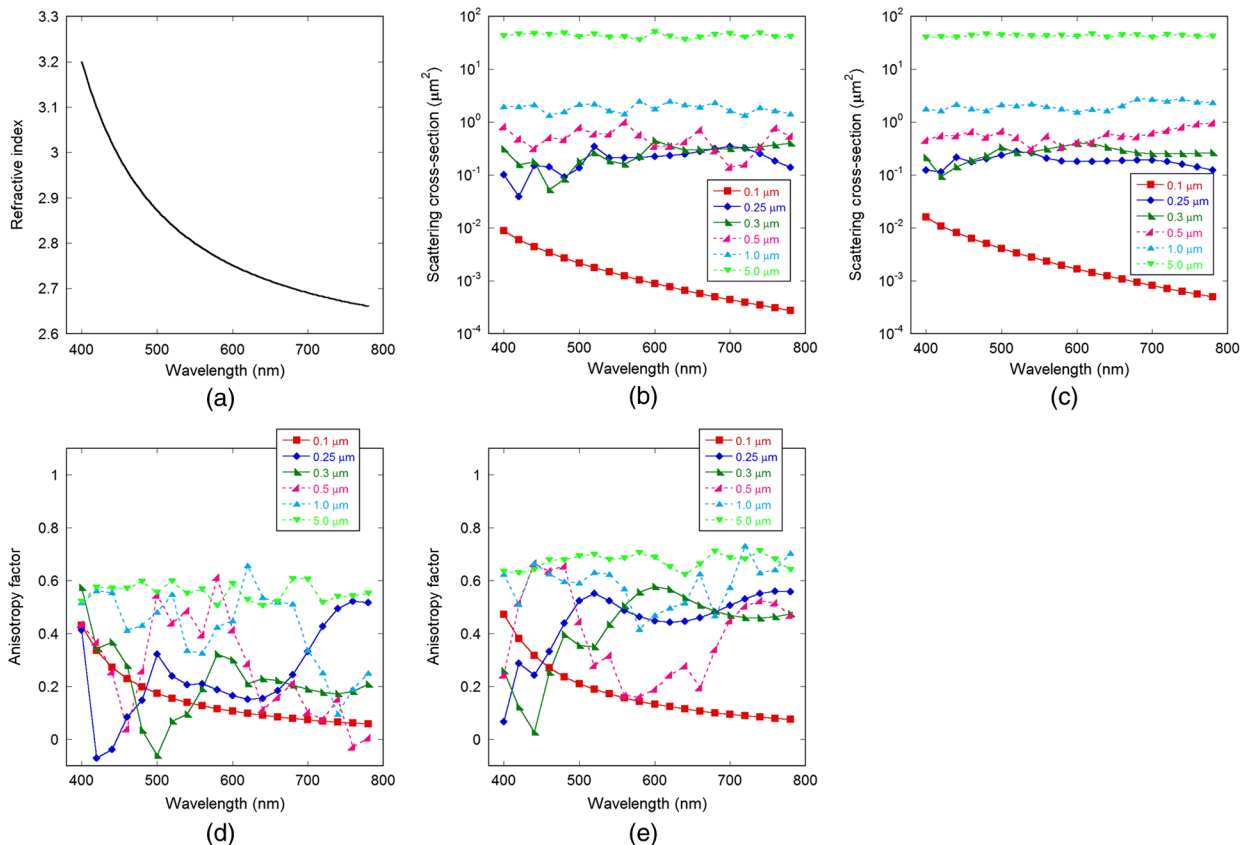


Fig. 3 (a) Refractive index, (b, c) scattering cross-section, (d, e) anisotropy factor g . The refractive index of the surrounding medium: (b), (d) 1.0 and (c), (e) 1.4.

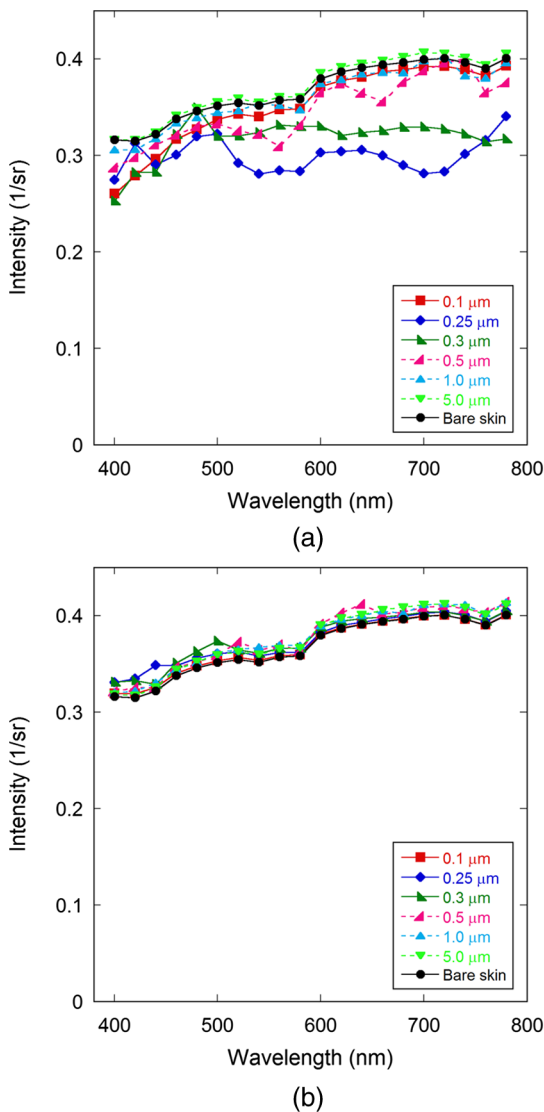


Fig. 4 Reflection spectra observed at angle 0-deg to 10-deg for skin with and without powder particles. The refractive index of the medium surrounding the particles is: (a) 1.0 and (b) 1.4.

than 1 for all particle diameters between 50 and 1000 nm (50 nm interval) and all wavelengths between 380 and 780 nm (20 nm interval). In real situations, however, some photons still may experience multiple scattering even for this low concentration of particles. For simplicity, we treat all scattering events as single scattering in the simulation. We also examined the situation where a thin clear layer of gel containing powder particles exists on the skin to simulate liquid foundations. A commonly used ingredient of liquid foundation is silicone, which has a refractive index of 1.397 to 1.403. Hence, the refractive index of gel was set to be 1.4. The gel layer was assumed to be a nonabsorbing medium, and the change in the lateral position of a photon packet was ignored, which arises when the photon packet propagates obliquely in the gel layer.

In our simulations, infinitely narrow photon beams (photon packets) irradiate the skin surface normally, at random positions within a circle of radius 5 mm. The number of incident photon packets is 10^7 . A photon packet first collides with a particle or the surface of the skin. The collision event is determined by a random number generated according to probabilities derived

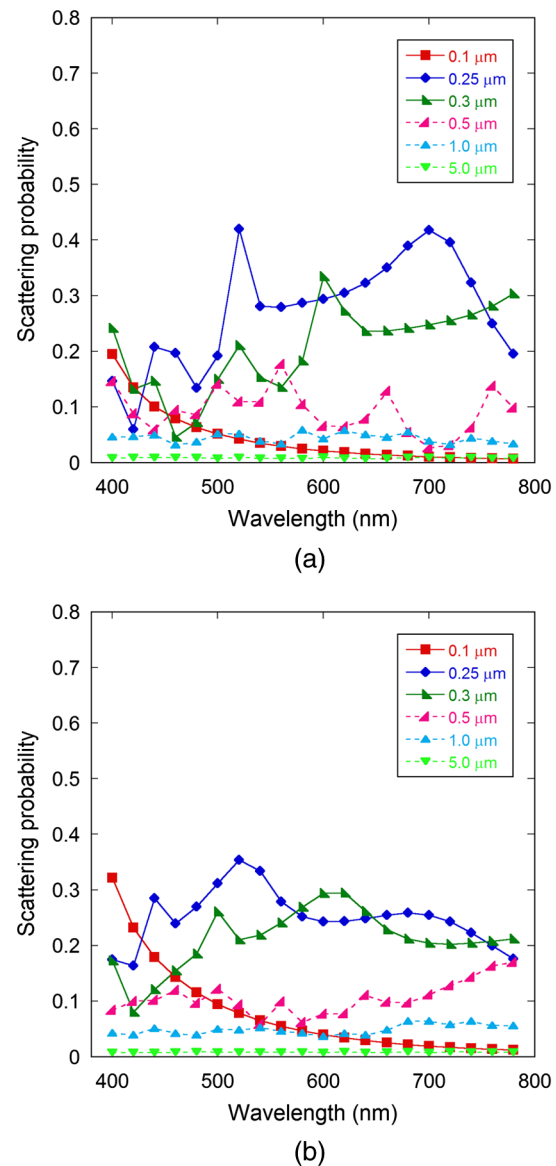


Fig. 5 Scattering probability of photons by particles. The refractive index of the medium surrounding the particles is: (a) 1.0 and (b) 1.4.

theoretically. The probability that a photon packet collides with a particle (scattering probability) is assumed to be given by $P = 1 - \exp(-\sigma_s N)$, where σ_s is the scattering cross-section of a particle and N is the number of particles per unit area (for more detailed discussion, see Appendix B). We fixed the mass of the particles per unit area, and hence, the probability P changes with the incident wavelength and the size and relative refractive index of a particle. If a photon packet is scattered by a particle, its direction is changed according to a random number, which obeys the angular probability distribution of scattered intensity (scattering phase function) derived from Mie scattering theory. If it hits the skin surface, it reflects from or penetrates into the layer of epidermis. Which event occurs is also determined by a random number generated in accordance with the Fresnel equations.

There are three main cases in which the photon packets do not enter the skin tissue: (1) they are backscattered by particles, (2) they impinge on the skin surface and are reflected back according to the Fresnel reflection, or (3) they are scattered

forward by particles and then reflected from the skin's surface. Multiple reflections between the particle layer and the skin surface are also taken into account; some photon packets undergoing the above discussed case 2 or 3 may hit a particle, are backscattered, reflected from the surface, scattered again by a particle, and so on. These components together constitute the surface reflected light. Although this bouncing of photon packets between particles and the skin surface is reasonable only when the particles are floating in a gel layer, the case for particles "suspended" in the air near skin surface has also been simulated to examine the effect of the surrounding medium alone. If the particles are in contact with the skin, a large number of multiple reflections of coherent light occur between the particles and the skin's surface, leading to a change in the surface reflectance and the angular distribution of the reflected light.¹⁹ When the powder is immersed in a gel layer, the Fresnel reflection from the interface between air and gel gets also incorporated into the simulation.

The photon packets entering the skin tissue experience scattering and absorption. We employ a standard Monte Carlo modeling of photon transport in multilayered tissues.⁷ In order to represent a situation where a spatial variation exists in the absorption coefficient of the epidermis, the standard MC code has been modified to specify the absolute lateral position of the skin layers and photon packets. The Henyey–Greenstein

function was used as a phase function to describe light scattering inside the skin tissues. The internally reflected radiation (diffuse reflectance) and the surface reflection from the skin and the particles were recorded at various observation angles (zenith angles) with 0-deg being the exact backscattering direction. The intensity at observation angles $\theta_1 - \theta_2$ represents the power of reflected light collected over zenith angles between θ_1 and θ_2 and all azimuthal angles and normalized by the solid angle of the corresponding spherical zone.

3 Results and Discussion

3.1 Effect of Powder Particles

First, we consider the effect of powder particles on the spectrum of light reflected from the skin. Figure 4(a) and 4(b) show the reflection spectra for skin covered with various sizes of particles that are surrounded by air and gel, respectively. The angle of observation is 0 deg through 10 deg. For the suspension medium of air, the shape of the spectrum changes dramatically from that of the bare skin for particles of size 0.25 and 0.3 μm diameters because of the complex wavelength dependence of Mie scattering for particles with a diameter comparable to the wavelength of light. Another reason for this is that the average scattering probability P is relatively high for these particle diameters [see Fig. 5(a)]: 27.3% for 0.25 μm and 20.8% for 0.3 μm , larger

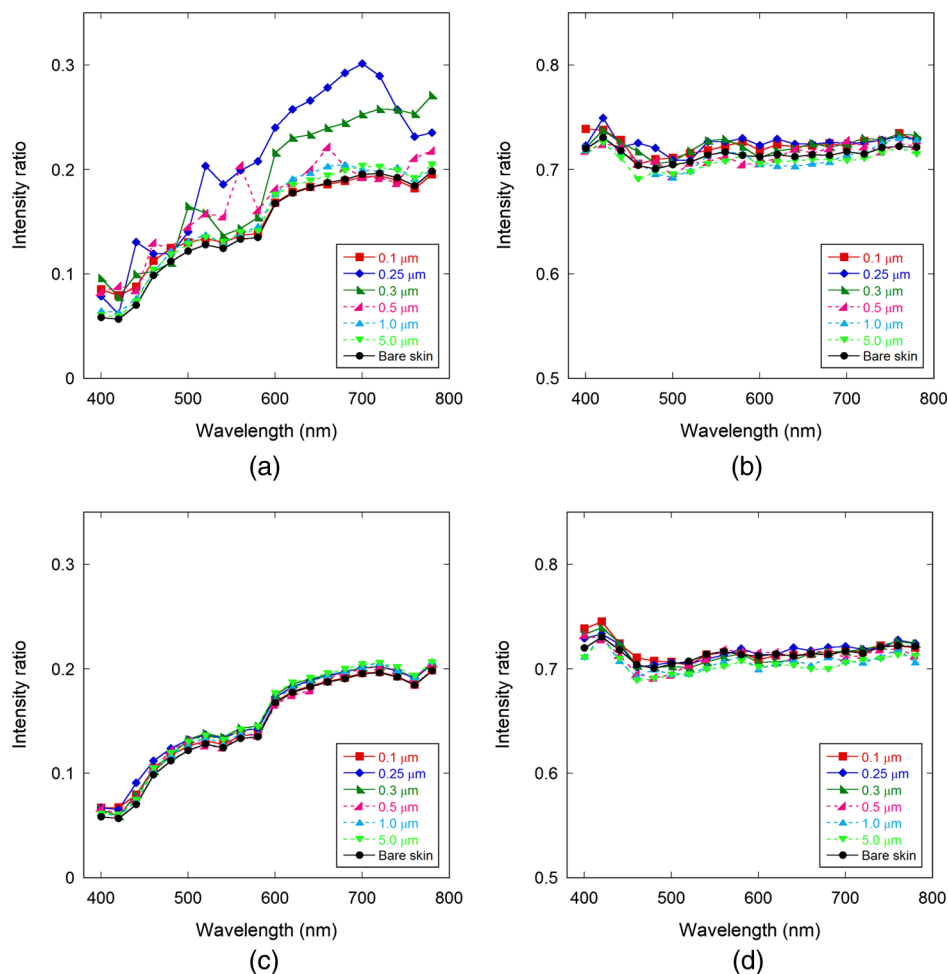


Fig. 6 Ratio of the intensity observed at 40-deg to 50-deg to that at 0-deg to 10-deg for (a) and (c): total reflected light and (b) and (d): internally reflected light. The refractive index of the medium surrounding the particles is: (a, b) 1.0 and (c, d) 1.4.

than those for other diameters (4.4, 9.3, 4.4, and 0.8% for 0.1, 0.5, 1.0, and 5.0 μm , respectively). Conversely, the spectral shape is almost preserved for 1.0 and 5.0 μm size particles. For these particles, the average anisotropy factor g is 0.42 and 0.56, for diameters 1.0 and 5.0 μm [see Fig. 3(d)], respectively, which are larger than those of other diameters (0.15, 0.25, 0.22, and 0.27 for 0.1, 0.25, 0.3, and 0.5 μm , respectively). The small scattering probability and the large anisotropy factor make application of large particles on skin less effective. The spectrum of 0.1 μm particles differs from that of bare skin only in the short wavelength region (<460 nm). In this region of the spectrum, the scattering probability increases as the wavelength becomes shorter for these small particles (probability less than 8% for wavelengths larger than 460 nm compared to 19.5% for 400 nm). The incident photons are then scattered away in other directions at short wavelengths, reducing the reflected intensity in the direction around 0-deg.

As seen from Fig. 4(b), embedding the particles in liquid or gel suppresses the spectral change caused by Mie scattering. The relative refractive index of the particles decreases by immersing the particles in a medium of refractive index larger than 1.0. While the scattering probability increases or decreases depending on the particle sizes, the anisotropy factor g increases for all the particles: for example, the value of g averaged for all wavelengths (400 to 780 nm) increases from 0.22 to 0.41, for 0.3 μm particles. Thus, the scattering strength of the particles decreases, weakening the effect of particles on the spectral reflectance.

The reflection spectrum of the skin depends on the angle of observation. As an example, the ratio of the intensity detected at an angle of 40-deg to 50-deg to that detected at 0-deg to 10-deg is shown in Fig. 6. We assume that the skin surface is flat so that photons are reflected from the bare skin surface only in the direction of 0-deg. The wavelength dependence for bare skin in Fig. 6(a) is caused mainly by the presence or absence of the Fresnel reflection, which is independent of the wavelength and included only in the intensity value at 0-deg to 10-deg, the denominator of the intensity ratio. The dependence of the spectrum on the observation angle varies according to the size of particles. In comparison with Fig. 4(a), it can be seen that the spectral peaks and valleys are reversed for particles with diameters less than 1.0 μm . This indicates that the particles that scatter less light within the scattering angle around exact backscattering tend to scatter more in other directions, and vice versa. It is shown from Fig. 6(b) that the spectral shape of internally reflected light depends minimally on the observation angle, even if spherical particles exist near the surface of the skin. These spectral changes of reflected intensity as a function of the observation angle are similar for the particles immersed in gel [Fig. 6(c) and 6(d)], although the relative magnitudes are small compared to that of air. We calculate the intensity ratio for other directions and confirm a similar tendency. Therefore, the variations in the intensity ratio of the total reflected light are mostly from the variations in the surface reflected light.

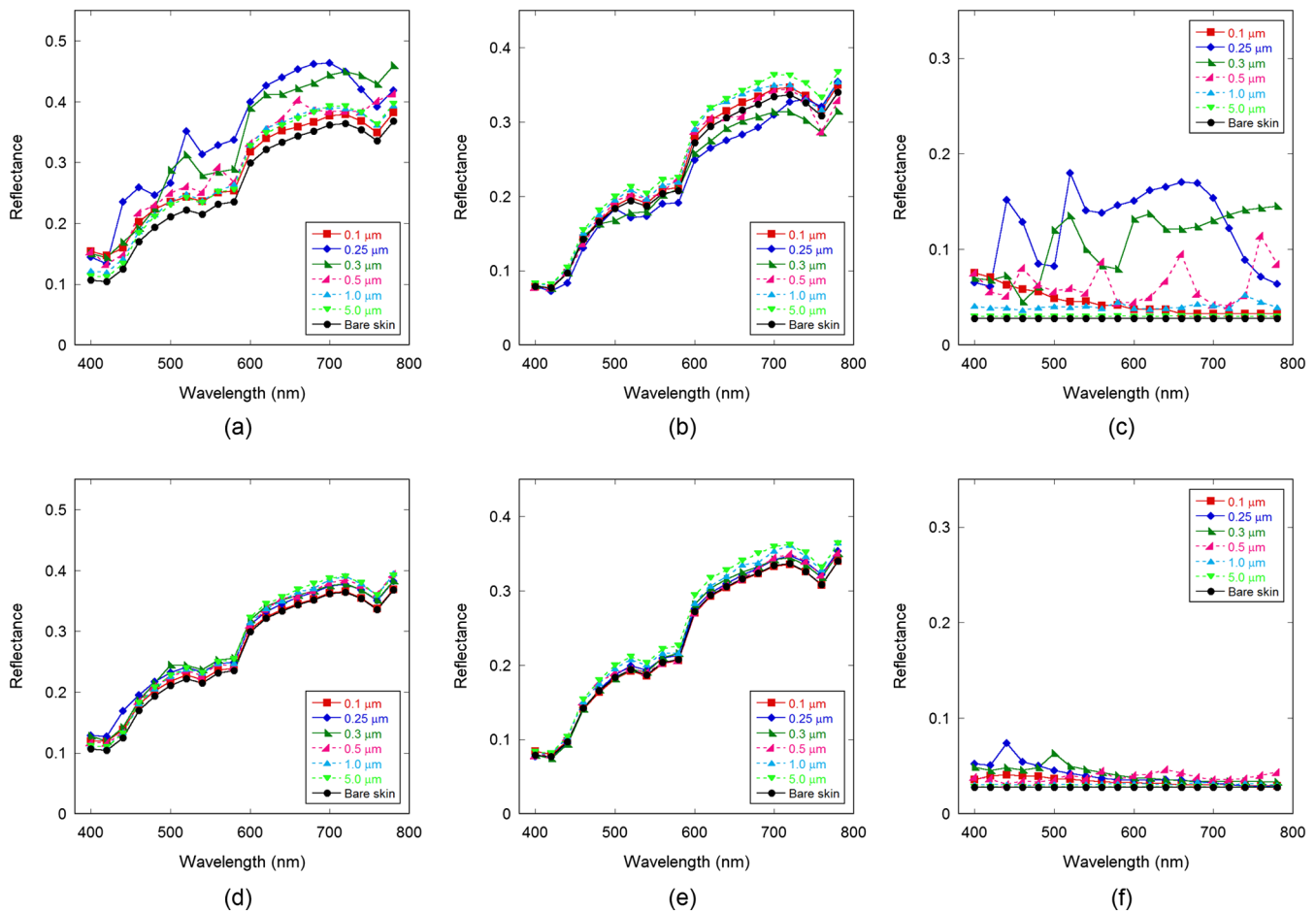


Fig. 7 Spectral reflectance for (a, d): total reflected light, (b, e): internally reflected light, and (c, f): surface reflected light. The refractive index of the medium surrounding the particles is: (a)–(c) 1.0 and (d)–(f) 1.4.

Next, we examine spectral reflectance, which is given by the total energy of light propagating in all backward directions normalized to the input light energy. In actual experiments, it is obtained by measuring the spectrum of backscattered light collected with an integrating sphere.¹¹ Figure 7(a) and 7(d) show the spectral reflectance for bare skin and skin with various particle sizes surrounded by air and gel, respectively. It is seen from Fig. 7(a) that the reflectance of total backscattered light is increased by the powder layer, especially for the 0.25 and 0.3 μm particles. For the 0.1 μm particles, mainly the short wavelength portion of light is reflected; this is because of the wavelength dependence of scattering probability and the small value of the anisotropy factor, as discussed before. However, particles of 1.0 and 5.0 μm diameters have little effect on the spectrum of total reflected light, similar to the tendency observed at a certain angle [Figs. 4(a) and 6(a)]. When the particles are surrounded by gel, the large reflectance otherwise exhibited by 0.25 and 0.3 μm particles is not observed, and only the spectral features of each particle remain.

The spectra of internally and surface reflected light shown in Fig. 7(b), 7(c), 7(e), and 7(f) demonstrate the contributions of surface reflection and internal reflection to the spectral reflectance in Fig. 7(a) and 7(d). A comparison of Fig. 7(a) with 7(c) and Fig. 7(d) with 7(f) reveals that the effect of powder particles appears mainly in the spectrum of the surface reflected light. In

particular, 0.25 and 0.3 μm particles in the air enhance the surface's reflection with distinctive spectral patterns, giving rise to larger total reflectance with unique wavelength dependence. Although surface reflected light increases for all particles, internally reflected light increases or decreases, depending on the particle size and the surrounding medium.

3.2 Powder on Discolored Skin

One of the purposes of cosmetic powder is to hide skin discoloration. We investigated the effect of powder particles on the appearance of skin color. Figure 8(a)–8(d) show color images of normal skin, pigmented skin, normal skin with a pigmented area on the left-hand side of the image, and half-pigmented skin covered with gel alone, respectively. These images were generated by transforming calculated spectra to XYZ tristimulus values and then by transforming them to corresponding RGB tristimulus values. The corresponding sRGB values were obtained from the RGB values, with overall gamma of 2.2. The pigmented skin was simulated by increasing the volume fraction of melanosomes from 5% to 10%, leading to relatively darker appearance than the normal skin, as shown in Fig. 8(b). The absorption coefficient of the epidermis was evaluated using the following equation:^{1,20}

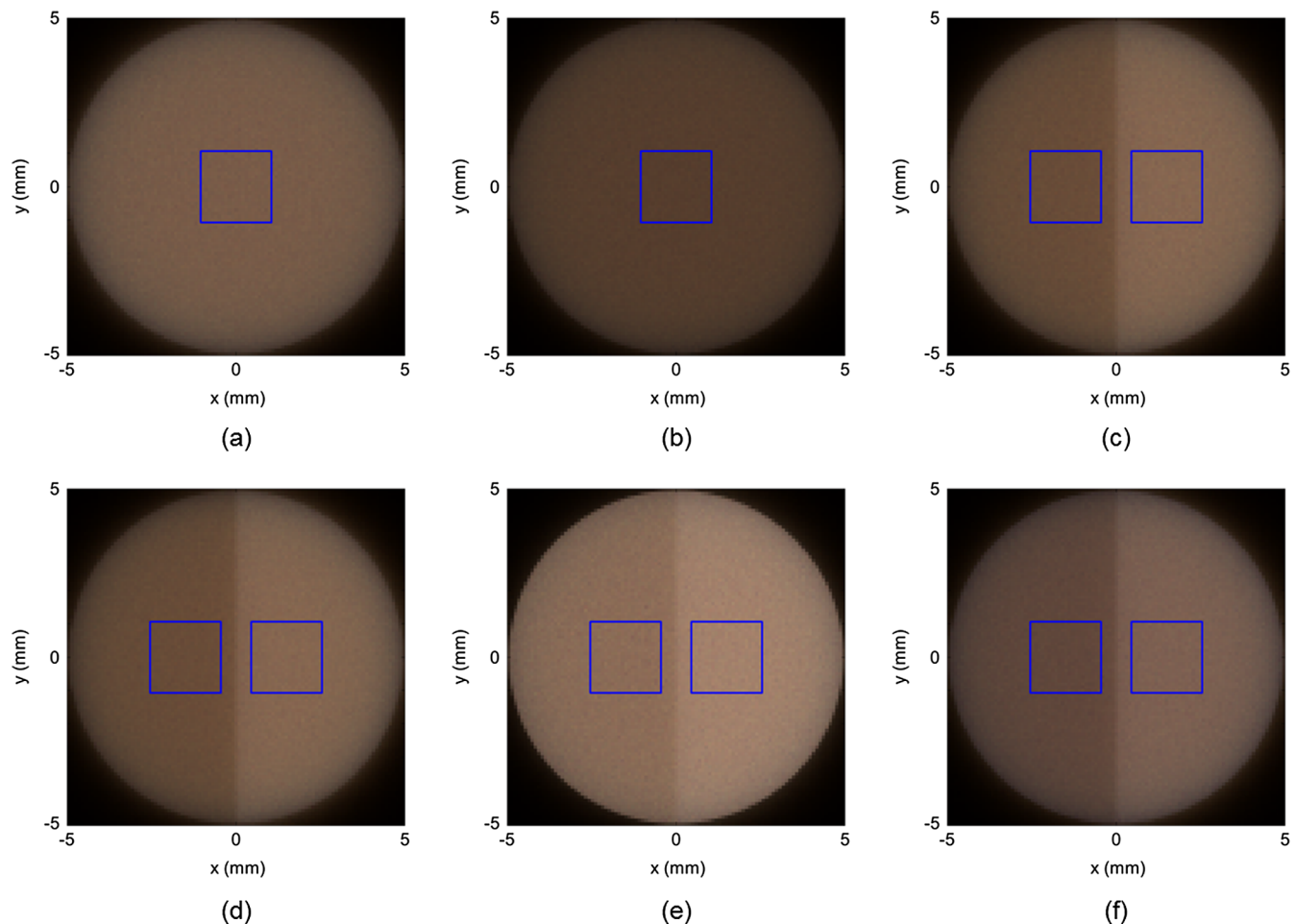


Fig. 8 Images of skin generated by the simulation. (a) normal bare skin, (b) pigmented bare skin, (c) bare skin with a pigmented area on the left half of the image, (d) half-pigmented skin covered with gel alone, (e) half-pigmented skin applied with 0.25- μm particles, and (f) half-pigmented skin covered with gel containing 0.25- μm particles. In (d)–(f), gel and/or particles are applied on both areas. Squares in the figures represent the area for which $L^*a^*b^*$ values in the CIELAB color scale are calculated.

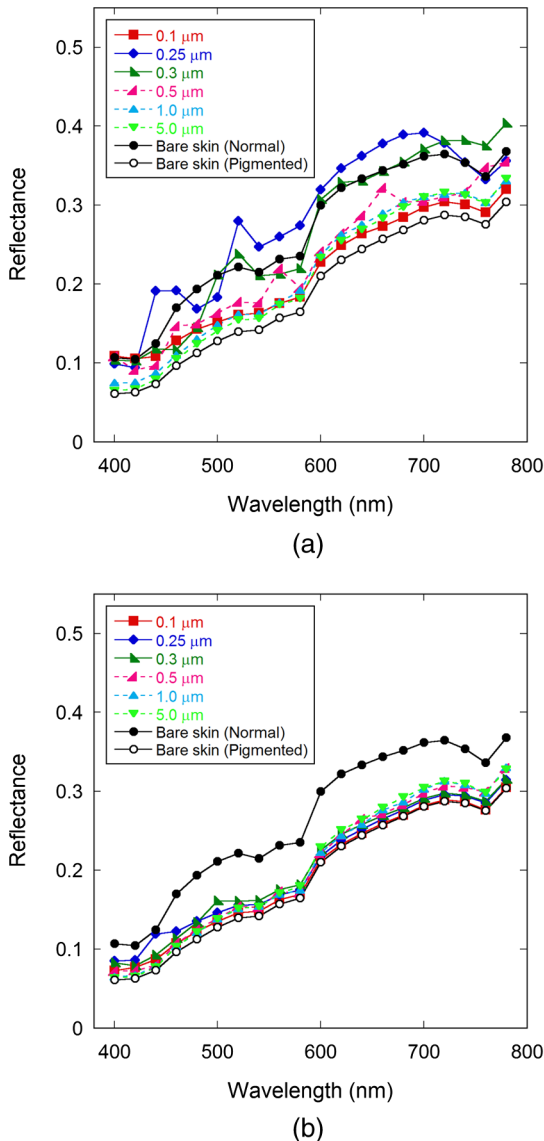


Fig. 9 Spectral reflectance for bare skin and discolored skin with various particle diameters. The refractive index of the medium surrounding the particles is (a) 1.0 and (b) 1.4.

$$\mu_{a,epi} = f_{mel} \cdot \mu_{a,mel} + (1 - f_{mel}) \cdot \mu_{a,skin},$$

where f_{mel} is the volume fraction of melanosomes, and $\mu_{a,mel}$ and $\mu_{a,skin}$ are the absorption coefficients of single melanosome and skin layer without melanin, respectively. The wavelength dependence of the absorption coefficient of the pigmented epidermis is shown in Fig. 2(a).

The spectral change in reflected light by applying powder particles on the discolored skin [Fig. 8(b)] is shown in Fig. 9. Comparing Fig. 9(a) and 9(b) with Fig. 7(a) and 7(d) shows that reflectance decreases while maintaining the spectral shapes, for all cases. Since the surface reflectance is independent of the absorption coefficient of the skin, it is the same value for the normal skin and discolored skin. Thus, a decrease in the reflectance stems from a reduction in internal reflection. As shown in Fig. 7(b), 7(c), 7(e), and 7(f), the characteristics of the spectrum are formed mostly by surface reflection and, therefore, spectral shape is minimally affected by any change in the amount of absorption. It should be noted, however, that the

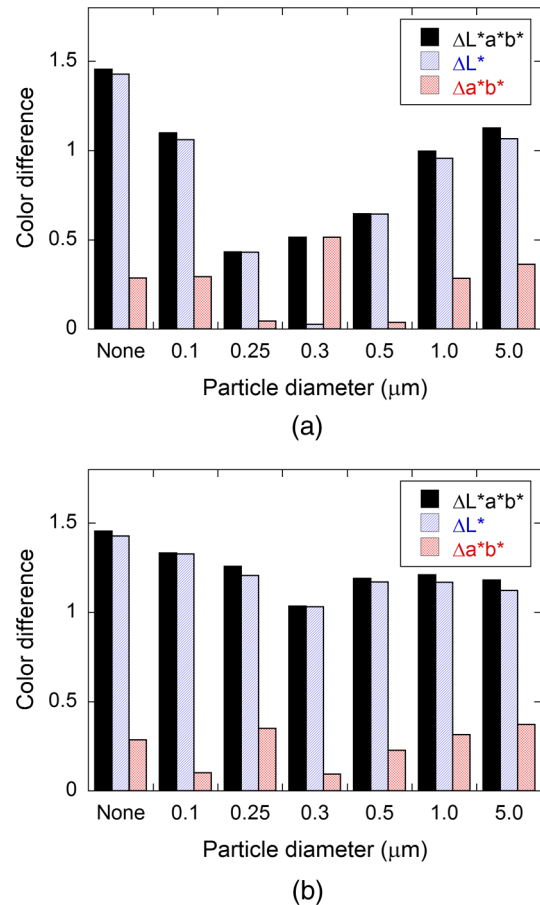


Fig. 10 Color difference between normal skin without particles and discolored skin with particles. The refractive index of the medium surrounding the particles is (a) 1.0 and (b) 1.4.

decrease in the ratio of reflectance becomes larger for shorter wavelengths. Light with short wavelengths cannot penetrate into deep skin, so that it is more influenced by absorption in the epidermis, compared to light with longer wavelengths.

In order to quantitatively examine the ability of TiO_2 powder to make skin pigmentation less noticeable, we consider the color difference between normal skin and discolored skin when the powder is applied. The $L^*a^*b^*$ values are calculated in the CIELAB color scale with a D_{65} light source, and the differences in color $\Delta L^*a^*b^*$, lightness ΔL^* and color phase Δa^*b^* between the normal skin and the discolored skin were evaluated, where $\Delta L^*a^*b^* = \sqrt{(\Delta L^*)^2 + (\Delta a^*b^*)^2}$. First, we compare the color of pigmented skin [Fig. 8(b)] covered with particles of various sizes with that of normal skin [Fig. 8(a)] without particles. This comparison shows whether covering the pigmented area with powder makes their color close to that of normal bare skin. The results are shown in Fig. 10, where the color differences measured in square regions in Fig. 8(a) and 8(b) are plotted for two refractive indices of the medium surrounding the particles. The case where no powder is applied on either the normal skin or the discolored skin is also presented (“none” in Fig. 10), which gives the reference criteria for the color differences. As shown in Fig. 10, the difference in lightness is much larger than that in color phase, when we compare the two types of bare skin. All the particles show the same tendency, except the $0.3 \mu\text{m}$ particles surrounded by the air. When the particles are in the air, the color difference $\Delta L^*a^*b^*$

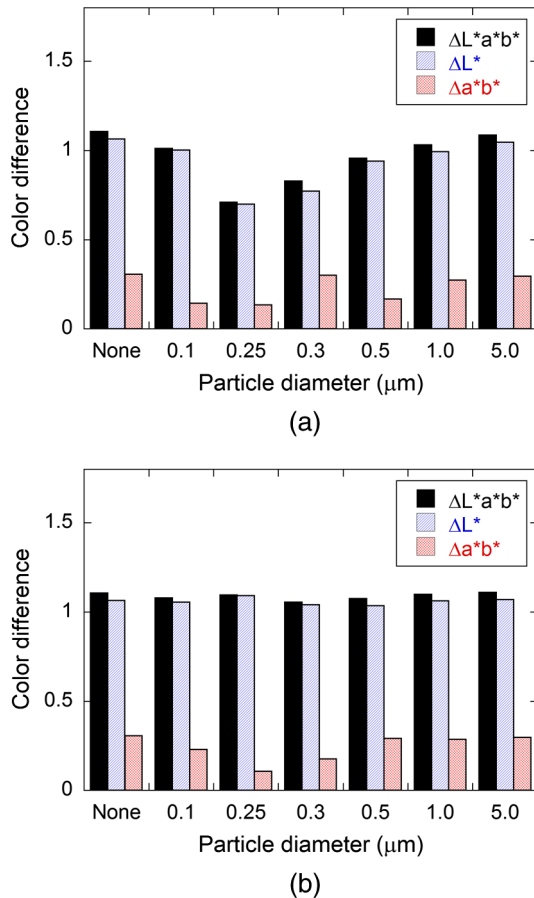


Fig. 11 Color difference between normal skin and discolored skin when particles cover both areas. The refractive index of the medium surrounding the particles is (a) 1.0 and (b) 1.4.

becomes small for the 0.25 and 0.3 μm particles, whereas the 0.1 and 5.0 μm particles give large $\Delta L^*a^*b^*$ values. In comparison with Fig. 9, this result suggests that, although the spectra for the 0.25 and 0.3 μm particles are different from that of normal bare skin, their reflectance values are close to those of normal bare skin, which makes the color difference smaller than that for the other sizes of particles. When the particles are in gel, the color difference is almost the same for all the particle sizes, except 0.3 μm . In both cases, although the difference in lightness ΔL^* behaves almost the same as $\Delta L^*a^*b^*$, the difference in color phase Δa^*b^* shows a different behavior. Low values of Δa^*b^* are obtained for 0.25 and 0.5 μm particles surrounded by air and 0.1 and 0.3 μm particles surrounded by gel. Therefore, the appearance of skin color is greatly affected by the refractive index of the medium in which powder particles are embedded.

Figure 11 shows the difference in color between two square regions in Fig. 8(c) and 8(d), where all the areas in Fig. 8(c) and 8(d) are covered with powder particles of the same size. This corresponds to the situation where the foundation is applied on the entire skin including a pigmented area. The particles with a diameter of 0.25 or 0.3 μm exhibit low color difference compared with that of the other diameters. This result is reasonable because, as shown in Fig. 7(c) and 7(f), the surface reflectances for these two types of particles are larger than that for the other particles, leading to a reduction in internal reflections from which the difference in color between normal and

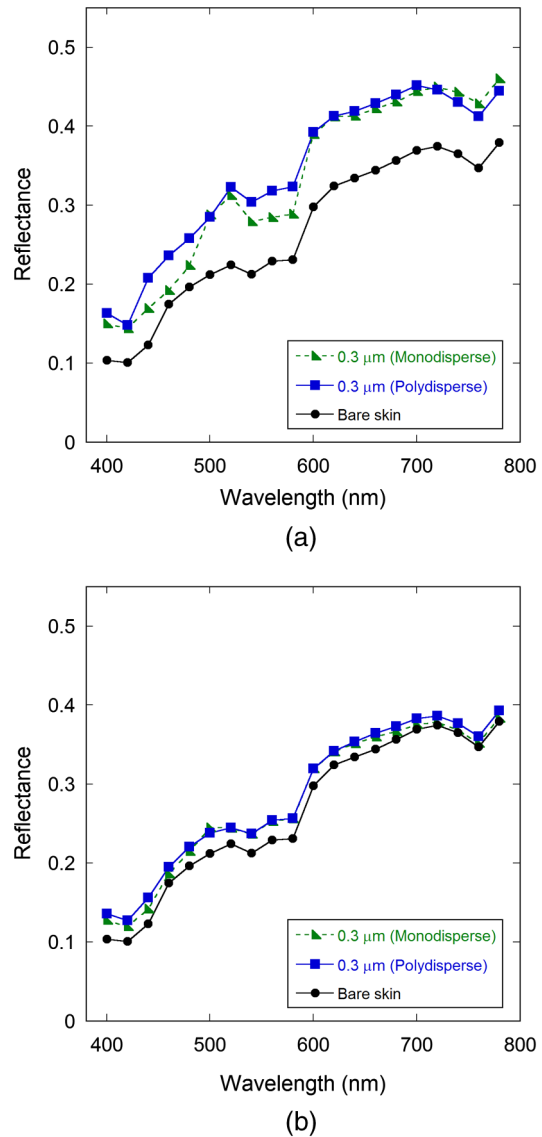


Fig. 12 Spectral reflectance for normal bare skin and normal skin covered with monodisperse and polydisperse particles. The refractive index of the medium surrounding the particles is (a) 1.0 and (b) 1.4.

discolored skin arises. As for the difference in color phase Δa^*b^* , the lowest values are obtained for 0.25 μm particles in both surrounding media. The corresponding color images are presented in Fig. 8(e) and 8(f), showing that the difference in color phase decreases compared with Fig. 8(c) and 8(d), respectively. Therefore, among the particles of various sizes we tested, particles with a diameter of 0.25 μm are more suitable for obscuring color imperfections on the skin. It is seen that the variations in color difference among different sizes of the particles are small compared with those presented in Fig. 10. This is because the target of comparison is normal skin with the same powder applied, not the normal bare skin as shown in Fig. 10. Interestingly, a comparison between the color differences for the bare skin in Figs. 10 and 11 (“none” in the figures) reveals that ΔL^* decreases in Fig. 11, while Δa^*b^* is almost the same. This decrease in the difference of lightness indicates that some of the photons incident on the normal skin area exit from the pigmented area, and vice versa, for the half-pigmented case in Fig. 8(c).

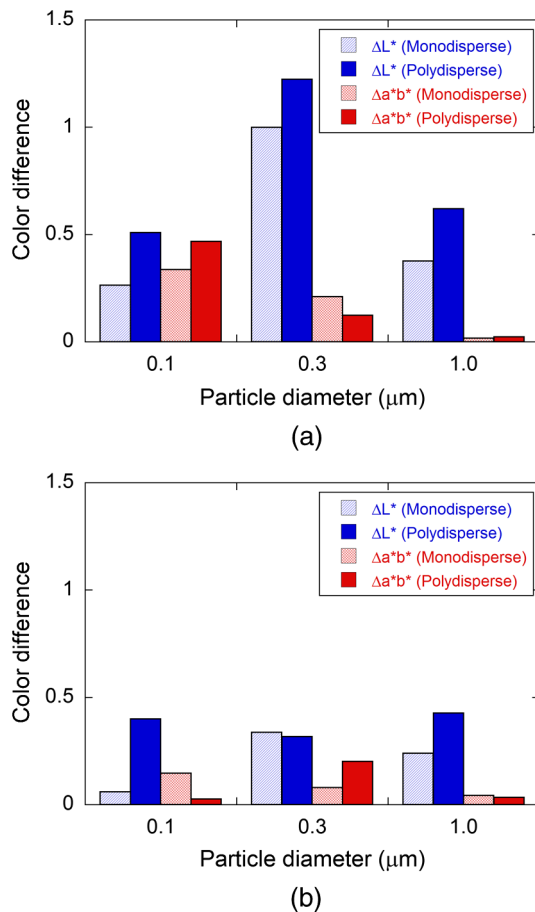


Fig. 13 Difference in lightness ΔL^* and color phase Δa^*b^* between normal bare skin and normal skin with monodisperse and polydisperse particles. The refractive index of the medium surrounding the particles is (a) 1.0 and (b) 1.4.

3.3 Effect of Polydispersity

When we consider the actual situations of light scattering from powder particles, it is appropriate to take into account a distribution of particle size, i.e., polydispersity. The effect of particle size distribution was examined using three average diameters of 0.1, 0.3, and 1.0 μm . The size distribution of particles is assumed to be log-normal in weight, and this distribution is approximated by a set of 11 different particle diameters, for each average size (see Appendix C for details). Figure 12 shows the reflection spectra obtained for 0.3 μm monodisperse and polydisperse particles, together with that for the normal bare skin. One can see that the characteristic spectral pattern for scattering from monodisperse particles, is substantially suppressed using polydisperse particles, and the shape of the spectrum approaches that of the bare skin.

The color difference between normal bare skin and normal skin with powder particles is shown in Fig. 13, for monodisperse

and polydisperse cases. It is seen that the difference in lightness ΔL^* increases appreciably for diameters of 0.1 and 1.0 μm , when the particles have a size distribution. As shown in Fig. 7(c) and 7(f), 0.25, 0.3, and 0.5 μm particles reflect light strongly with their own spectral preferences. The polydisperse particles with average sizes of 0.1 and 1.0 μm contain particles with diameters larger than 0.1 μm and smaller than 1.0 μm , respectively. These submicrometer particles make the brightness of the skin more different from that of bare skin. The difference ΔL^* for the 0.3 μm polydisperse particles increases less than that of the other two for the surrounding medium of air, and decreases for gel. As for the difference in color phase, the value of Δa^*b^* increases or decreases, depending on the average particle size and the surrounding medium. This result indicates a complex behavior that is shown in Fig. 10 for monodisperse particles with various sizes.

4 Conclusions

In this study, a simulation model was developed for light scattering and reflection from three-layer-structured skin covered with powder particles. This MC-based model provides spectral reflectance data at a specific angle of incidence and at a specific angle of observation. We used a phase function for an isolated spherical particle, assuming that the effects of light interference between particles and the skin surface and among particles are negligible. This assumption can be relaxed in future investigations by employing the phase functions that take into account the influence of the skin surface and neighboring particles.^{19,21,22} Particles with shapes other than spherical can also be simulated, if their scattering phase functions are known beforehand.

Using our model, we analyzed the reflection spectrum of light for various particle sizes and discussed their spectral characteristics. The results show that the spectrum of reflected light changes by changing the observation angle, reflecting the shape of the Mie scattering phase function of monodisperse particles present near the surface of the skin. The color difference between the light reflected from normal and discolored skin was then analyzed to examine the cover-up effect of powder particles. Among various particle sizes we examined, particles with a diameter of 0.25 μm are suitable to cover up discoloration of the skin. This is because the total scattering cross-section of this size of particles is relatively large, under the condition of a constant mass for the powder applied. In addition, the intensity of light backscattered from these particles is relatively large owing to the small value of the anisotropy factor g . It should be noted, however, that a smaller difference in color does not always imply more natural skin appearance: increased surface reflection leads to a corresponding reduction of the internal reflection that makes the skin look fresh and healthy. It is, therefore, important to develop a simulation model capable of realistically representing the powder particles, to achieve a perfect balance between covering up imperfections of the skin and giving it a natural and healthy look.

Table 1 Number of particles per unit area for monodisperse particles.

Diameter (μm)	0.1	0.25	0.3	0.5	1.0	5.0
Number density (cm^{-2})	2.42×10^9	1.55×10^8	8.95×10^7	1.93×10^7	2.42×10^6	1.93×10^4

Table 2 Number of particles per unit area for polydisperse particles.

Average diameter (μm)	0.1		0.3		1.0	
	Diameter (μm)	Number density (cm^{-2})	Diameter (μm)	Number density (cm^{-2})	Diameter (μm)	Number density (cm^{-2})
	0.02	1.09×10^3	0.1	4.29×10^4	0.4	8.17×10^3
	0.04	1.92×10^7	0.15	4.34×10^6	0.55	2.18×10^5
	0.06	5.48×10^8	0.2	2.78×10^7	0.70	8.07×10^5
	0.08	1.34×10^9	0.25	4.25×10^7	0.85	1.03×10^6
	0.1	9.01×10^8	0.3	2.80×10^7	1.0	6.81×10^5
	0.12	2.88×10^8	0.35	1.10×10^7	1.15	2.96×10^5
	0.14	5.99×10^7	0.4	3.12×10^6	1.3	9.82×10^4
	0.16	9.75×10^6	0.45	7.29×10^5	1.45	2.74×10^4
	0.18	1.38×10^6	0.5	1.50×10^5	1.6	6.80×10^3
	0.2	1.82×10^5	0.55	2.87×10^4	1.75	1.57×10^3
	0.22	2.78×10^4	0.6	6.81×10^3	1.9	3.73×10^2

Appendix A: Optical Parameters of Skin Layers and Powder Particles

The three optical parameter values of skin layers for normal and discolored skin used in the simulation are plotted as a function of wavelength, in Fig. 2. The only difference between normal and discolored skin is the difference in the absorption of light in the epidermis.

The various optical parameter values of the particles used in the simulation are plotted as a function of wavelength in Fig. 3. It should be noted that, in some cases, the scattering cross-section can be larger for smaller contrast of the refractive index between particles and the surrounding medium (particles of 0.1 μm diameter, for example).

Appendix B: Scattering Probability of Photons by Powder Particles

The scattering probability P of photons in the particle layer is given by:

$$P = 1 - \exp(-\tau) = 1 - \exp(-\mu_s L), \quad (1)$$

where τ , L and μ_s are the optical depth, the thickness and the scattering coefficient of the layer, respectively. The scattering coefficient is defined as:

$$\mu_s = \sigma_s \rho, \quad (2)$$

where σ_s is the scattering cross-section of a particle ρ and is the number of particles per unit volume (volume density). When particles are applied on the skin in an area A , all the particles exist in a volume AL . Since the volume density of particles is given by:

$$\rho = N/AL, \quad (3)$$

where N is the number of particles. The probability of scattering is rewritten as:

$$P = 1 - \exp(-\sigma_s \rho L),$$

and after substitution we get:

$$P = 1 - \exp\left[-\sigma_s \left(\frac{N}{AL}\right) L\right].$$

Simplifying we get:

$$P = 1 - \exp\left(-\frac{\sigma_s N}{A}\right). \quad (4)$$

If A is set to be 1 (cm^{-2}), N corresponds to the number of particles per unit area (cm^{-2}). Therefore, the scattering cross-section and the area density of particles determine the scattering probability. The number density of particles is given in Table 1, where N is evaluated from the specific weight of TiO_2 (4.26 g/cm^3) and the concentration of particles (5.39 $\mu\text{g}/\text{cm}^2$). Equation (4) is calculated using the value of the scattering cross-section [Fig. 3(b) and 3(c)] for each wavelength and particle diameter. Figure 5 shows the scattering probability plotted for various particle sizes with different refractive indices of the surrounding medium.

Appendix C: Polydispersity of Particles

Polydisperse particles were modeled based on the size distribution of typical TiO_2 particles commonly used for makeup foundations. First, a log-normal cumulative distribution was fitted to the cumulative weight distribution of the particle size frequency distribution of the TiO_2 particles. Then, derivatives were taken at eleven different particle sizes and the weigh percent of each size of the particles was calculated. Finally, the number of

particles of each size was evaluated so that the total weight of the particles is equal to $5.39 \mu\text{g}/\text{cm}^2$. The number density of particles used in the simulation are shown in Table 2.

References

1. T. Igarashi, K. Nishino, and S. K. Nayar, "The appearance of human skin: a survey," *Found. Trends Comput. Graph. Vis.* **3**(1), 1–95 (2007).
2. G. V. G. Baranoski and A. Krishnaswamy, *Light & Skin Interactions: Simulations for Computer Graphics Applications*, Morgan Kaufmann, New York (2010).
3. P. Kubelka, "New contributions to the optics of intensely light-scattering materials. Part I," *J. Opt. Soc. Am.* **38**(5), 448–457 (1948).
4. P. Kubelka, "New contributions to the optics of intensely light-scattering materials. Part II: Nonhomogeneous layers," *J. Opt. Soc. Am.* **44**(4), 330–335 (1954).
5. B. C. Wilson and G. Adam, "A Monte Carlo model for the absorption and flux distributions of light in tissue," *Med. Phys.* **10**(6), 824–830 (1983).
6. V. V. Tuchin, S. R. Utz, and I. Y. Yaroslavsky, "Tissue optics, light distribution, and spectroscopy," *Opt. Eng.* **33**(10), 3178–3188 (1994).
7. L. Wang, S. L. Jacques, and L. Zheng, "MCML—Monte Carlo modeling of photon transport in multi-layered tissues," *Comput. Meth. Prog. Biomed.* **47**(2), 131–146 (1995).
8. I. V. Meglinski and S. J. Matcher, "Computer simulation of the skin reflectance spectra," *Comput. Meth. Prog. Biomed.* **70**(2), 179–186 (2003).
9. N. Tsumura et al., "Regression-based model of skin diffuse reflectance for skin color analysis," *Opt. Rev.* **15**(6), 292–294 (2008).
10. R. Eze and S. Kumar, "Laser transport through thin scattering layers," *Appl. Opt.* **49**(3), 358–368 (2010).
11. T. Maeda et al., "Monte Carlo simulation of spectral reflectance using a multilayered skin tissue model," *Opt. Rev.* **17**(3), 223–229 (2010).
12. I. Nishidate et al., "Noninvasive imaging of human skin hemodynamics using a digital red-green-blue camera," *J. Biomed. Opt.* **16**(8), 086012 (2011).
13. A. P. Popov et al., "Effect of size of TiO₂ nanoparticles embedded into stratum corneum on ultraviolet-A and ultraviolet-B sun-blocking properties of the skin," *J. Biomed. Opt.* **10**(6), 064037 (2005).
14. A. P. Popov et al., "The effect of nanometer particles of titanium oxide on the protective properties of skin in the UV region," *J. Opt. Technol.* **73**(3), 208–211 (2006).
15. A. P. Popov et al., "Effect of multiple scattering of light by titanium dioxide nanoparticles implanted into a superficial skin layer on radiation transmission in different wavelength ranges," *Quantum Electron.* **37**(1), 17–21 (2007).
16. A. P. Popov et al., "Biophysical mechanisms of modification of skin optical properties in the UV wavelength range with nanoparticles," *J. Appl. Phys.* **105**(10), 102035 (2009).
17. I. Nishidate, Y. Aizu, and H. Mishina, "Estimation of absorbing components in a local layer embedded in the turbid media on the basis of visible to near-infrared (VIS-NIR) reflectance spectra," *Opt. Rev.* **10**(5), 427–435 (2003).
18. J. R. DeVore, "Refractive indices of rutile and sphalerite," *J. Opt. Soc. Am.* **41**(6), 416–419 (1951).
19. A. Garcia-Valenzuela, E. Gutierrez-Reyes, and R. G. Barrera, "Multiple-scattering model for the coherent reflection and transmission of light from a disordered monolayer of particles," *J. Opt. Soc. Am. A* **29**(6), 1161–1179 (2012).
20. S. L. Jacques, "Skin optics," <http://omlc.ogi.edu/news/jan98/skinoptics.html> (10 May 2013).
21. G. Videen, "Light scattering from a sphere on or near a surface," *J. Opt. Soc. Am. A* **8**(3), 483–489 (1991).
22. G. Videen, "Light scattering from a sphere behind a surface," *J. Opt. Soc. Am. A* **10**(1), 110–117 (1993).